AGU PUBLICATIONS

JGR

Journal of Geophysical Research: Space Physics

RESEARCH ARTICLE
10.1002/2015JA022123

Key Points:
- Six year statistics of the similarity of Pc1 pearl structures at longitudinally and latitudinally separated induction magnetometers
- Generation mechanism of Pc1 pearl structures in the ionosphere
- Dependence of the similarity of Pc1 pearl structures on UT, month, year, and geomagnetic conditions

Correspondence to:
C.-W. Jun,
chae-woo@isee.nagoya-u.ac.jp

Citation:
Jun, C.-W., K. Shiokawa, M. Connors, I. Schofield, I. Poddelsky, and B. Shevtsov (2016), Possible generation mechanisms for Pc1 pearl structures in the ionosphere, based on 6 years of ground observations in Canada, Russia, and Japan, *J. Geophys. Res. Space Physics*, *121*, 4409–4424, doi:10.1002/2015JA022123.

Received 5 NOV 2015
Accepted 25 APR 2016
Accepted article online 2 MAY 2016
Published online 21 MAY 2016

Possible generation mechanisms for Pc1 pearl structures in the ionosphere based on 6 years of ground observations in Canada, Russia, and Japan

Chae-Woo Jun[1], Kazuo Shiokawa[1], Martin Connors[2], Ian Schofield[2], Igor Poddelsky[3], and Boris Shevtsov[3]

[1]Institute for Space-Earth Environmental Research, Nagoya University, Nagoya, Japan, [2]Center for Science, Athabasca University, Athabasca, Canada, [3]Institute of Cosmophysical Research and Radiowave Propagation, Far Eastern Branch of the Russian Academy of Sciences, Vladivostok, Russia

Abstract We investigate pearl structures (amplitude modulations) of Pc1 pulsations simultaneously observed at Athabasca (ATH, 54.7°N, 246.7°E, $L = 4.3$) in Canada, Magadan (MGD, 60.1°N, 150.7°E, $L = 2.6$) in Russia, and Moshiri (MOS, 44.4°N, 142.3°E, $L = 1.5$) in Japan. From 6 years of ground observations, from 2008 to 2013, we selected 84 Pc1 events observed simultaneously at the longitudinally separated stations (ATH and MGD) and 370 events observed at the latitudinally separated stations (MGD and MOS), all with high coherence (>0.7) of Pc1 waveforms. We calculated the cross-correlation coefficient (similarity: r) for the Pc1 pearl structures and found that more than half of the events in both pairs had low similarity ($r < 0.7$), indicating that most Pc1 waves exhibit different pearl structures at different stations. We found that high-similarity Pc1 pearl structures ($r > 0.7$) at the longitudinally separated stations are concentrated from 6 to 15 UT when both stations are in the nighttime. The similarity of Pc1 pearl structures tends to show a negative correlation with the standard deviation of the polarization angle in both pairs. The observed repetition period of Pc1 pearl structures has a clear positive correlation with the repetition period estimated from Pc1 bandwidth by assuming beating of different frequencies. From these results, we suggest that ionospheric beating effect could be a dominant process for the generation of Pc1 pearl structures. Beating processes in the ionosphere with a spatially distributed ionospheric source can cause the different shapes of Pc1 pearl structures at different observation points during ionospheric duct propagation.

1. Introduction

Electromagnetic ion cyclotron (EMIC) waves are known to be generated in L shells 4 to 8 in the equatorial regions of the magnetosphere by ion cyclotron instabilities with an anisotropic energy distribution. Theoretical studies [e.g., *Horne and Thorne*, 1993] and observations [e.g., *Anderson et al.*, 1996] have suggested that EMIC waves are left-hand polarized Alfvén waves located near the generation region in the magnetosphere. They propagate by bouncing along the magnetic field lines between the Southern and Northern Hemispheres. During this bouncing motion, some portion of EMIC wave energy passes through the ionospheric resonance region, allowing the waves to propagate into the ionosphere [*Fraser*, 1975a, 1975b; *Altman and Fijalkow*, 1980; *Fujita*, 1988]. In the ionosphere, right-hand polarized compressional (fast) isotropic waves are generated through the interaction of the incident EMIC waves with the ionospheric plasma in the *F* region. Theory and observations show that after this mode conversion from Alfvén to compressional waves, the compressional waves can be trapped in the ionospheric duct (or waveguide) centered on the F_2 region (a layer of maximum electron density at an altitude of ~400 km) with minimum Alfvén speed [e.g., *Manchester*, 1966; *Tepley and Landshoff*, 1966; *Campbell*, 1967; *Kuwashima et al.*, 1981; *Kawamura et al.*, 1981; *Kim et al.*, 2011; *Waters et al.*, 2013]. These trapped waves propagate latitudinally and longitudinally from the ionospheric source region to low latitudes. These waves are observed on the ground as Pc1 pulsations in the frequency range of 0.2–5 Hz as classified by *Jacobs and Watanabe* [1964] and *Fukunishi et al.* [1981]. During ionospheric duct propagation, the wave energy of Pc1 pulsations is attenuated with an attenuation ratio of 0 to 13 dB/1000 km [*Althouse and Davis*, 1978; *Kim et al.*, 2010]. In previous studies, Pc1 pulsations were frequently observed at high latitudes during the daytime with a maximum occurrence at 1 to 2 h before sunrise during winter. On the other hand, the occurrence of Pc1 pulsations at low latitudes peaked during the nighttime about 1 h after local magnetic noon and during equinoxes [*Fraser*, 1968; *Kuwashima et al.*, 1981].

"Pc1 pearl structures" are a phenomenon in Pc1 pulsations, which have a quasiperiodic amplitude modulations in the repetition period of several tens of seconds [*Troitskaya and Gul'Elmi*, 1967]. To investigate mechanisms for the generation of Pc1 pearl structures, there have been many studies using ground-based and satellite observations [e.g., *Perraut*, 1982; *Erlandson et al.*, 1990; *Guglielmi et al.*, 1996; *Mursula et al.*, 1997; *Rasinkangas and Mursula*, 1998; *Mursula et al.*, 1999; *Mursula*, 2007; *Usanova et al.*, 2008; *Nomura et al.*, 2011; *Jun et al.*, 2014]. To explain the generation of Pc1 pearl structures, we consider two possibilities: (1) magnetospheric effects and (2) ionospheric effects.

One candidate magnetospheric effect is encapsulated in the bouncing wave packets (BWP) model [e.g., *Guglielmi et al.*, 1996; *Mursula et al.*, 1999]. The model suggests that the bouncing of EMIC waves along the magnetic field lines between the Northern and Southern Hemispheres causes Pc1 pearl structures. According to this model, the length of magnetic field line associated with EMIC wave sources could be a main controller for the repetition period of Pc1 pearl structures. Because the Alfvén velocity in the magnetosphere has a dependence on plasma conditions along the field line, the travel time of these wave packets between hemispheres is related to the repetition periods. According to this theory, the repetition period of Pc1 pearl structures would have a connection with the length of the magnetic field lines. This period would vary in the range of several tens of seconds due to the location of the EMIC generation region near the magnetospheric equator. However, some studies have suggested to reconsider whether or not the BWP model is a good one for the formation of Pc1 pearl structures. For example, their repetition periods may significantly differ from the results expected from this model [e.g., *Perraut*, 1982; *Paulson et al.*, 2014]. If Pc1 pearl structures are mainly caused by BWP model, the repetition period in space should be half of that on the ground. However, comparing ground and satellite observations, *Perraut* [1982] found that the repetition periods of Pc1 pearl structures observed in space did not bear this relationship to those on the ground. Furthermore, *Paulson et al.* [2014] observed repetition periods on the ground that were similar to those in space. Additionally, using data obtained by the Viking satellite near the plasmapause, *Erlandson et al.* [1990] found that the Poynting flux of Pc1 pearl structures was mainly directed downward, along the magnetic field lines, into the ionosphere.

Another magnetospheric effect that is a candidate for Pc1 pearl generation is the modulation of EMIC waves by long-period ULF waves (such as Pc4-Pc5 pulsations), which was suggested by *Mursula et al.* [2001] and *Mursula* [2007]. They found that EMIC waves observed in space were modulated by magnetospheric Pc3 pulsations. The generation of Pc1 pulsations by ion cyclotron instability also causes other amplitude modulations, such as EMIC rising tone emissions [*Omura et al.*, 2010; *Shoji and Omura*, 2013; *Nakamura et al.*, 2014]. It has also been suggested that Pc1 pearl structures can be generated by the superposition of EMIC waves traveling in the magnetosphere with a coherence length associated with the waves' growth [*Hu and Denton*, 2009].

Some studies have instead suggested beating processes in the ionosphere for the generation of Pc1 pearl structures [e.g., *Pope*, 1964; *Nomura et al.*, 2011; *Jun et al.*, 2014]. Beating in the ionosphere considers that Pc1 waves with slightly different frequencies associated with an extended north-south ionospheric source region are superposed at the observation points. The propagation time differences from extended sources to the ground stations can cause beating within their frequency ranges and generate different amplitude modulations at different observation points. Pc1 pearl structures may thus have different shapes at different locations on the ground due to different conditions of wave beating. *Pope* [1964] suggested that Pc1 pearl structures could be generated by the superposition of Pc1 waves with a broad frequency range during ionospheric duct propagation. *Nomura et al.* [2011] found that Pc1 polarization angle has a frequency dependence for about ~70% of Pc1 pulsations observed at low-latitude ground stations, suggesting that the Pc1 ionospheric source is spatially extended. *Sakaguchi et al.* [2008] found that the isolated proton auroral spots associated with Pc1 pulsations had longitudinal extents of 250–800 km. *Jun et al.* [2014] found that in the case of Pc1 pulsations from spatially extended ionospheric sources, Pc1 pearl structures were different at the three stations used in this study. This suggests that beating processes in the ionosphere could contribute to generate Pc1 pearl structures while these waves are propagating through the ionospheric duct. However, a statistical study of Pc1 pearl structures using multipoint ground stations has not been made until now.

Thus, even though many previous studies have investigated the formation of Pc1 pearl structures, a mechanism for their generation has not been found. We emphasize that this paper is the first statistical report on the similarity of Pc1 pearl structures simultaneously observed at multipoint ground-based induction magnetometers, including a 6 year period from 2008 to 2013, a half solar cycle from minimum to maximum. We selected Pc1 events with high coherence of Pc1 waveforms (>0.7), indicating that the Pc1 pulsations observed

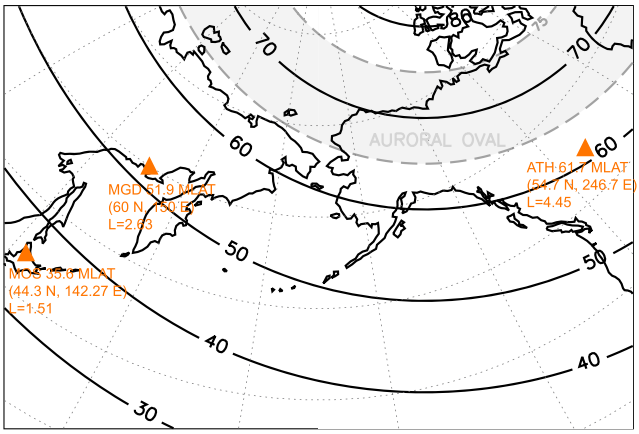

Figure 1. Locations of the three induction magnetometer stations: Athabasca (ATH) in Canada, Magadan (MGD) in Russia, and Moshiri (MOS) in Japan. Solid lines indicate dipole magnetic latitudes calculated using the IGRF-11 model with an epoch time of 2010. Dashed lines indicate geographic coordinates.

at different stations came from the same source region. In this paper, we study temporal characteristics and dependences of Pc1 pearl structures at longitudinally and latitudinally separated ground stations. If magnetospheric effects are dominant in the creation of Pc1 pearl structures, these structures should not change their shape during ionospheric duct propagation. However, if ionospheric effects are dominant, the structures may have different shapes when they are observed at different ground stations. In this paper, we report that even though they came from the same source, more than half of the events have low similarity ($r < 0.7$) of Pc1 pearl structures. We conclude that ionospheric beating effect during duct propagation could be the dominant process in Pc1 pearl generation.

2. Instrument Description

In this statistical analysis of Pc1 pearl structures in the ionosphere, we used longitudinally and latitudinally distributed induction magnetometers installed by the Solar-Terrestrial Environment Laboratory, Nagoya University, at Athabasca (ATH, 54.7°N, 246.7°E, $L = 4.3$) in Canada, Magadan (MGD, 60.1°N, 150.7°E, $L = 2.6$) in Russia, and Moshiri (MOS, 44.4°N, 142.3°E, $L = 1.5$) in Japan. The geographic coordinates (latitudes and longitudes) and dipole geomagnetic latitudes, obtained by the International Geomagnetic Reference Field (IGRF)-11 model using an epoch time of 2010, of these stations are shown in Figure 1. The stations are separated by approximately 5317 km for ATH and MGD and 1880 km for MGD and MOS. We record the three components (H, D, and Z) of the geomagnetic field provided by all three magnetometers. We use a sampling rate of 64 Hz, and the observation time is given by a GPS system with accuracy of ~1 μs. The magnetometer sensors have been calibrated by a 2 m coil by taking into account frequency sensitivities and phase differences, for all components, within Pc1 frequency range of 0.2–5.0 Hz. In addition, the magnetometer data were converted from volts to nanoteslas. More information on these induction magnetometers is provided by *Shiokawa et al.* [2010].

2.1. Analysis Methods and Event Selection

In this study, we used the H and D geomagnetic components obtained by induction magnetometers. Power spectrum density (PSD) is calculated for each component every 15 s with a time window of 64 s (4096 data points). The final frequency resolution is 0.0156 Hz. Figure 2 shows schematic pictures of the meaning of the coherence of Pc1 waveforms, the cross correlation of the upper envelopes of Pc1 amplitudes, and the standard deviation of Pc1 polarization angles. To examine if Pc1 waves observed at different observation points propagated from the same ionospheric source region, we calculated the coherence $C(\omega)$ of Pc1 waveforms with same time window of PSD using their waveforms as described in *Hino* [1977] (black solid curves shown in Figure 2a):

$$C_{xy}(\omega)^2 = \frac{\left|S_{xy}(\omega)\right|^2}{S_{xx}(\omega)S_{yy}(\omega)} \quad (1)$$

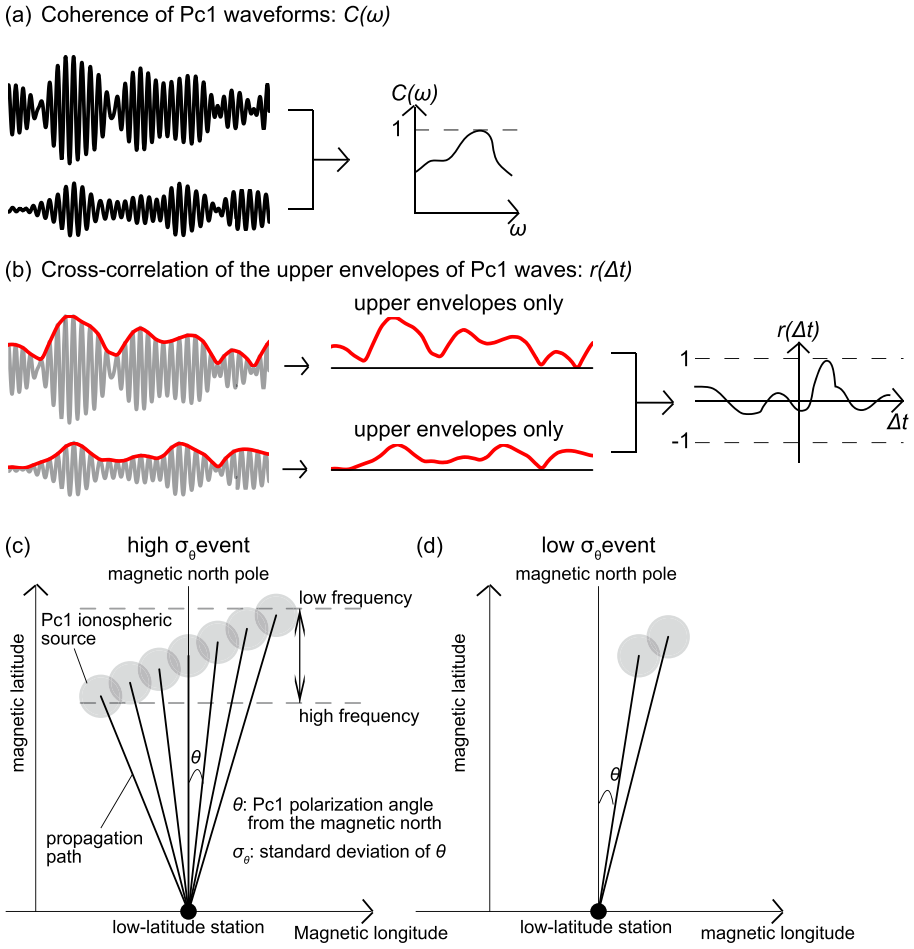

Figure 2. Schematic figures showing the meaning of (a) coherence of Pc1 waveforms $C(\omega)$, (b) cross-correlation of the upper envelopes of Pc1 waves $r(\Delta t)$, and standard deviation of polarization angle σ_θ ((c) high σ_θ event and (d) low σ_θ event).

where $S_{xx}(\omega)$ and $S_{yy}(\omega)$ are the PSDs for time series $x(t)$ and $y(t)$, respectively, and $S_{xy}(\omega)$ is the cross-spectrum density. If the coherence of the Pc1 waveforms between two stations is close to 1, then these signals are identical, indicating that they come from the same source. However, there is no relationship between two signals, if the coherence of Pc1 waveforms is close to zero, indicating that they have different sources. We calculated four pairs of $C(\omega)$ between stations: between $H_{Station1}$ and $H_{Station2}$; between $H_{Station1}$ and $D_{Station2}$; between $D_{Station1}$ and $H_{Station2}$; and between $D_{Station1}$ and $D_{Station2}$. From all of these cases, we selected the best pair satisfying our criteria (given below) to define the frequency range.

To identify whether the ionospheric source extended over a range of longitudes, we also calculated the standard deviation of the polarization angle (σ_θ) for the high-coherence Pc1 events only (Figures 2c and 2d). In each time window, we calculated the polarization angle (θ) as described by *Fowler et al.* [1967]. The angle (θ) is defined to be positive as measured westward from magnetic north. *Nomura et al.* [2011] found that the polarization angle has a dependence on Pc1 frequency. As Pc1 frequency is determined by local magnetic field intensity in the equatorial source region of the magnetosphere, an ionospheric source with a low (high) frequency of Pc1 pulsation would be located at higher (lower) latitudes. We assumed that a large (small) σ_θ would represent a spatially extended (localized) ionospheric source.

For this statistical study, we selected Pc1 pulsations observed simultaneously at two stations during a 6 year period, from 1 January 2008 to 31 December 2013, at the longitudinally (ATH and MGD) and latitudinally (MGD and MOS) separated stations. To select Pc1 pulsations observed simultaneously at the two stations, we used four selection criteria. First, the Pc1 pulsations must have a wave power higher than 10^{-7} nT^2/Hz in the dynamic spectra by visual inspection, in order to distinguish Pc1 pulsations from the background noise.

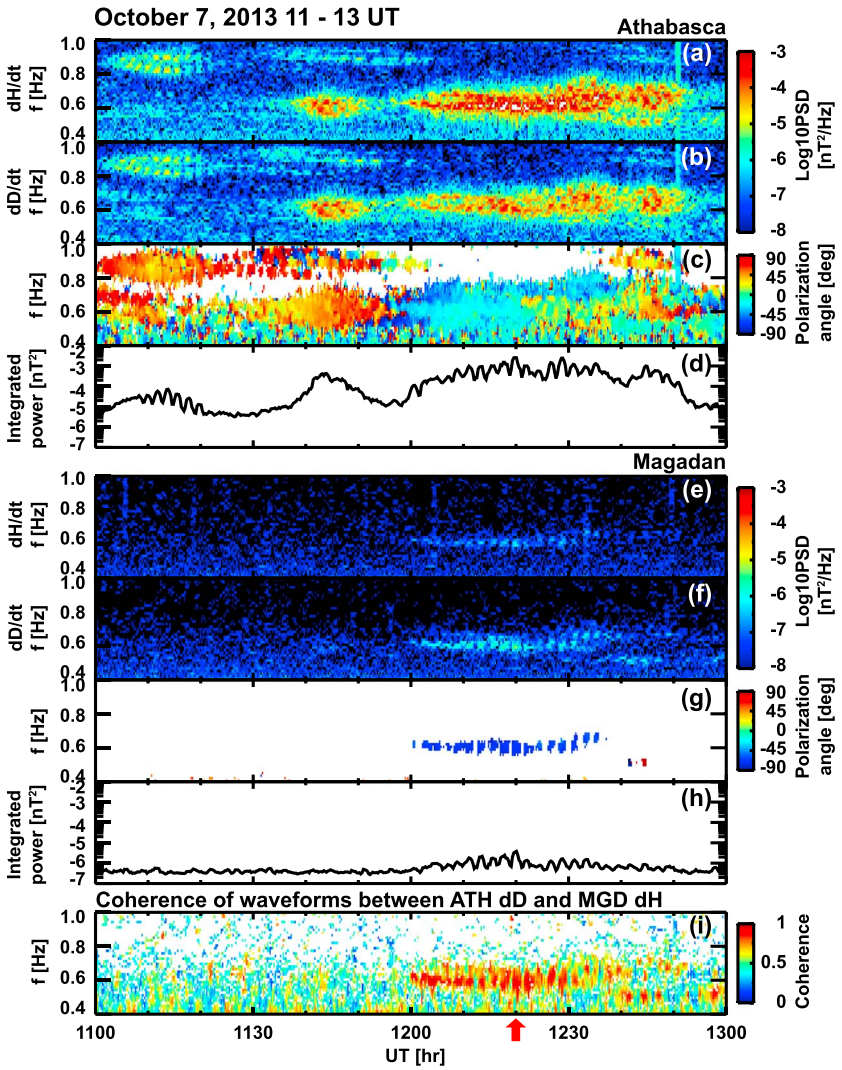

Figure 3. Dynamic spectrum densities of the (a) *H* and (b) *D* components of the magnetic field at ATH; (e) *H* and (f) *D* components of the magnetic field at MGD; (c) polarization angle at ATH and (g) at MGD; (d) the integrated wave power at ATH and (h) at MGD; (i) coherence of waveforms between ATH *D* and MGD *H* observed for 1100–1300 UT on 7 October 2013, in a frequency range of 0.4–1 Hz. The vertical arrows indicate the times 1219–1221 UT for which the power PSD and the waveforms of the magnetic field are shown in Figures 3 and 4, respectively.

Second, we take into account only high-coherence (>0.7) waveforms to consider Pc1 waves came from the same source region. Third, to identify clear characteristics of each Pc1 event, we used only the timing with the highest integrated Pc1 power at both stations (within the Pc1 frequency range). Then we used the averaged values of (σ_θ), central frequency, bandwidth, and auroral electrojet (*AE*) index within ±2 min of the selected timing, in order to obtain a representative value of these parameters of each event.

To define the similarity of Pc1 pearl structures between two different stations, we also calculated cross correlation ($r(\Delta t)$) of the upper envelopes of Pc1 amplitudes, red solid curves shown in Figure 2b. For this calculation, in order to consider all possibility of propagation of Pc1 pulsations through the ionospheric duct from high to low latitudes, we applied the maximum propagation time delay between two stations based on the minimum ionospheric duct propagation speed. Previous studies [*Greifinger and Greifinger*, 1968; *Manchester*, 1970; *Fraser*, 1975a; *Lysak*, 2004; *Kim et al.*, 2010] have suggested that the Alfvén speed of Pc1 pulsations in the ionosphere should be between 89 and 2000 km/s depending on ionospheric conditions. So in this study, we chose a maximum propagation time delay of ±59.7 s at the longitudinally separated stations (ATH and MGD) and ±21.1 s at the latitudinally separated stations (MGD and MOS) using the lowest propagation speed in the ionosphere (89 km/s).

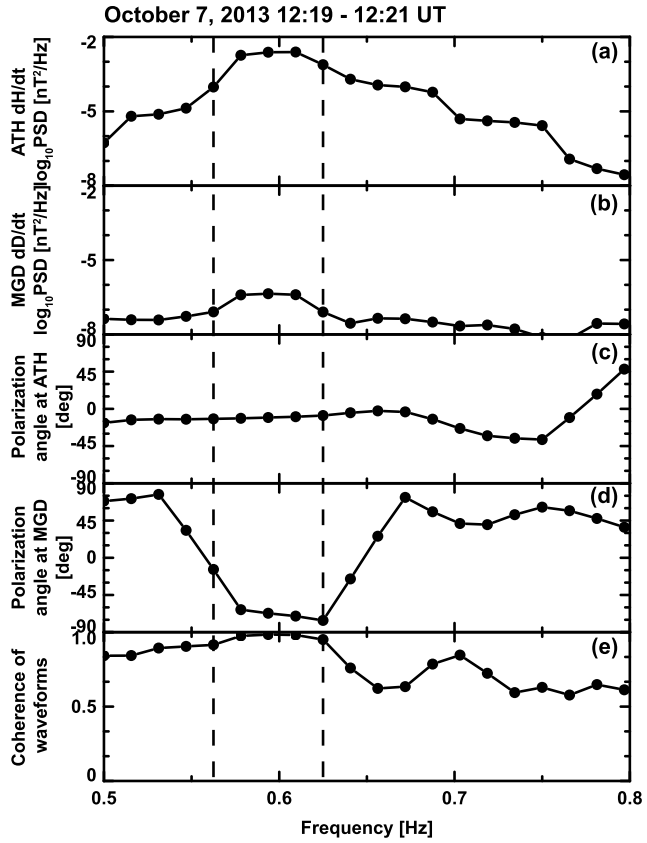

Figure 4. Power spectrum density of (a) the *H* component of the magnetic field at ATH and (b) the *D* component of the magnetic field at MGD, as well as (c) the coherence of Pc1 waveforms between the *H* component at ATH and *D* component at MGD, observed for 1219–1221 UT on 7 October 2013, in a frequency range of 0.5–0.8 Hz. The vertical dashed lines indicate the selected frequency range of 0.55 to 0.63 Hz, which satisfied our selection criteria.

Using these criteria, we selected 84 simultaneous Pc1 events at the longitudinally separated stations and 370 events at the latitudinally separated stations from the full 6 year data set. More than 86% of the 84 events for ATH-MGD gave the highest cross-correlation r with time differences Δt less than 20 s, corresponding to a propagation velocity higher than 265 km/s. More than 94% of the 370 events for MGD-MOS gave the highest cross-correlation r with time differences Δt less than 6 s, corresponding to a propagation velocity higher than 313 km/s.

2.2. Example of Event Selection: 7 October 2013

We illustrate our event selection using an event observed on 7 October 2013, between 11 and 13 UT at ATH and MGD. The dynamic spectra for *H* and *D* magnetic field components, the polarization angle, and the integrated wave power within the Pc1 frequency range is shown in Figure 3 for ATH (Figures 3a–3d) and MGD (Figures 3e–3h). The local time was 3 to 5 LT at ATH and 20 to 22 LT at MGD. During this time interval, *AE* index varied from 49 to 171 nT, indicating a weak substorm interval (not shown in the paper). In this time interval, we can see well-defined Pc1 pulsations observed at both stations. In Figures 3a–3d and 3e–3f, several Pc1 pulsations are shown clearly at both stations within the frequency range of 0.4 to 1 Hz. Pc1 pulsations observed at ATH can be separated into four time intervals with different frequency ranges: 0.8 to 1 Hz at 1100–1117 UT, 0.8 to 1 Hz at 1130–1200 UT, 0.5 to 0.7 Hz at 1140–1150 UT, and finally, 0.5 to 0.7 Hz at 1200–1250 UT. For MGD, Pc1 pulsations are observed at 1200–1240 UT within a frequency range of 0.5 to 0.7 Hz. The first three Pc1 bursts can be clearly seen at ATH as shown in Figure 3a–3b, but they are not simultaneously detected at MGD. As shown in Figure 3i, $C(\omega)$ between the *H* component magnetic field variations at ATH and the *D* component at MGD is close to 0 during these three time intervals. Thus, we exclude those intervals from our final event list.

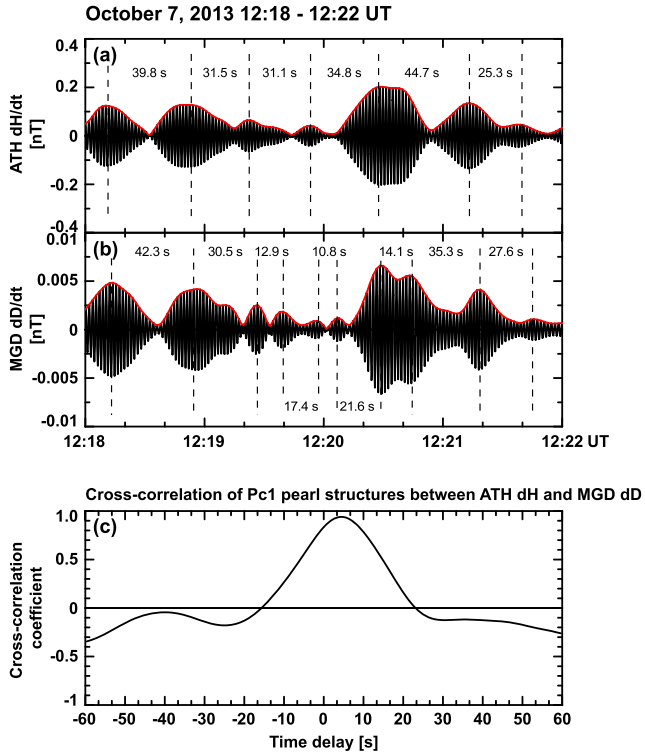

Figure 5. Band-pass filtered (0.55–0.63 Hz) Pc1 waveform of the magnetic field at (a) ATH (D component) and (b) MGD (H components) for 1218–1222 UT on April 8, 2010. Red solid lines indicate the upper envelope of the Pc1 pearl structures. (c) Cross-correlation between ATH D and MGD H components, obtained using the upper envelope of the Pc1 pearl structures.

From the above considerations, we focus on the Pc1 event observed simultaneously at both stations at 1200–1240 UT within frequency range of 0.5 to 0.7 Hz with high $C(\omega)$ (>0.7). In Figures 3c and 3g, the angles θ at ATH and MGD are shown, respectively. For ATH (Figure 3c), it suddenly changed from approximately −20° (bright blue) to +20° (green) at 1220 UT. For MGD (Figure 2g), the polarization angle was almost constant, with values around −60° (dark blue) with same frequency range as ATH at 1200–1240 UT. In this time interval, $C(\omega)$ between ATH d*D* and MGD d*H* (Figure 3i) is close to 1, suggesting that the observed Pc1 pulsations at both stations came from the same source region.

To investigate the similarity of Pc1 pearl structures at the two stations and its dependence on wave properties (i.e., central frequency, bandwidth, and standard deviation of polarization angle), we selected the time with the highest integrated Pc1 power at both stations. Figure 4 shows the averaged PSD of ATH d*H* and MGD d*D*, the polarization angle at ATH and MGD, and the coherence of Pc1 waveforms between the two stations at 1219–1221 UT on 7 October 2013 (resolution of 0.0156 Hz). At ATH (Figure 4a), a continuous high-PSD band existed at frequencies of 0.5 to 0.75 Hz. At MGD (Figure 4b), however, we see a narrow low-PSD band at frequencies of 0.58 to 0.63 Hz above 10^{-7} nT^2/Hz shown by the vertical dashed lines. $C(\omega)$ between the two stations is close to 1 in the latter frequency range. We also see a slight dependence of polarization angle on frequency at the two stations. In Figures 4c and 4d, the polarization angle varied from −11.5° to −8.11° at ATH and from −62.8° to −75.8° at MGD in the frequency range of 0.58 to 0.63 Hz. Using these values, we calculated σ_θ in order to investigate the distribution of the ionospheric source regions. In this event, σ_θ at ATH and MGD are 1.77° and 16.89°, respectively.

To investigate the similarity of Pc1 pearl structures in the ionosphere, we calculated $r(\Delta t)$ between ATH and MGD. Figure 5 shows the waveforms of the *H* component of Pc1 pulsations at ATH and the *D* components at MGD on 7 October 2013, at 1218–1222 UT. To separate noise from the other frequencies, a band-pass filter is applied for frequencies between 0.55 and 0.63 Hz. This frequency range has the highest coherence of waveforms between the two stations. We see a clear modulation of Pc1 amplitudes, red solid curves in Figure 5a and 5b, with repetition periods of 25.3–44.7 s at ATH and 10.8–42.3 s at MGD. The average repetition

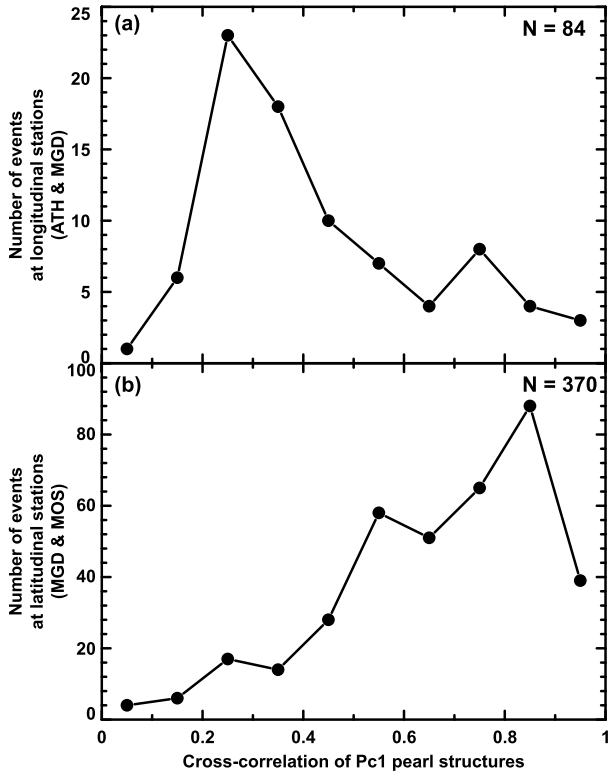

Figure 6. Distribution of similarity of Pc1 pearl structures observed at (a) longitudinally (ATH and MGD) and (b) latitudinally (MGD and MOS) separated stations.

periods at ATH and MGD are 34.6 s and 23.6 s, respectively. These modulations are the Pc1 pearl structures. In Figure 5c, the maximum cross-correlation coefficient between these envelopes is close to 1 ($r \sim 0.94$) with a time difference of approximately 4.3 s, indicating that ATH observed Pc1 amplitude modulations 4.3 s earlier than MGD.

3. Statistical Analysis

Using 84 Pc1 events observed simultaneously at the longitudinally separated stations (ATH and MGD) and 370 events at the latitudinally separated stations (MGD and MOS), we investigated statistical characteristics of the Pc1 pearl structures in the ionosphere. In this section, we show the distribution of similarity of Pc1 pearl structures, temporal variations of Pc1 occurrence, and similarity of Pc1 pearl structures, as well as their dependence on geomagnetic conditions and wave properties.

3.1. Distribution of Similarity of Pc1 Pearl Structures

Figure 6 shows the distribution of the similarity of Pc1 pearl structures at the longitudinally (ATH and MGD) and latitudinally (MGD and MOS) separated stations. We found that pearl similarity r has peaks at ~0.2 at the longitudinally separated stations (ATH and MGD, Figure 6a), and at ~0.8 the latitudinally separated stations (MGD and MOS, Figure 6b). *Jun et al.* [2014] reported that Pc1 pearl structures caused by beating processes in the ionosphere have slightly different shapes in model calculations of Pc1 pearl structures. Note that more than half of the events in both pairs (69 events at the longitudinally separated stations and 178 at the latitudinal stations) have similarities of less than 0.7. For the latitudinally separated stations, we detected simultaneous Pc1 events approximately four times more often than at the longitudinally separated stations. This difference of Pc1 occurrence may be related to attenuation effects during ionospheric duct propagation [*Althouse and Davis*, 1978].

3.2. Temporal Variations of Similarity of Pc1 Pearl Structures in the Ionosphere

Figure 7 shows the UT dependence of the occurrence of Pc1 pulsations observed at two stations and the similarity of Pc1 pearl structures in the ionosphere. The occurrence rate is calculated as the duration of the Pc1

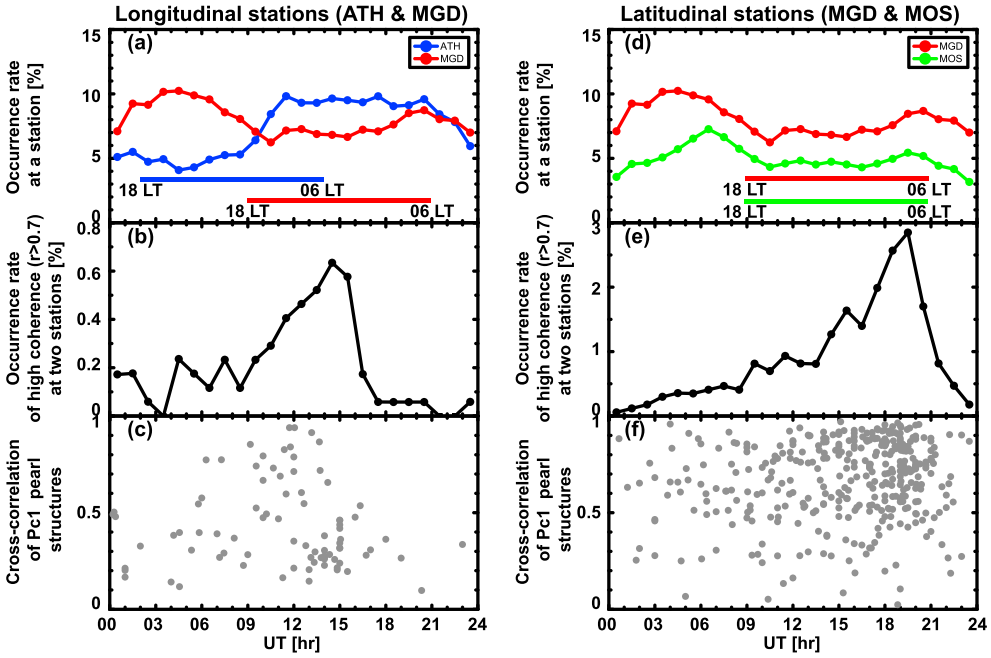

Figure 7. Daily variations of the Pc1 occurrence rate observed at each station, at the two stations, and the cross-correlation coefficient of Pc1 pearl structures for (a–c) longitudinally (ATH and MGD) and (d–f) latitudinally (MGD and MOS) separated stations, respectively. The horizontal colored bars in Figures 7a and 7d indicate local night time at ATH (blue), MGD (red), and MOS (green).

event divided by the total observation time. In Figures 7a and 7d, Pc1 pulsations observed at ATH have a peak occurrence in the morning sector. On the other hand, for MGD and MOS the peak is in the daytime. The occurrence rates of Pc1 pulsations at ATH and MGD are consistent with previous statistical studies on the ground [e.g., *Fraser*, 1968; *Kawamura et al.*, 1981; *Kuwashima et al.*, 1981]. These studies suggest that the occurrence rate of Pc1 pulsations observed at high latitudes (low latitudes) has a maximum during the daytime and up to 1 h after magnetic local noon (during the nighttime and up to 1 h before sunrise) probably due to the ionospheric electron density profile in the *F* region. However, the peak occurrence rate for MOS, located in the afternoon, differs from that found in previous studies.

Figure 7b shows that the occurrence rate of Pc1 pulsations observed simultaneously at the longitudinally separated stations has a clear peak around 15 UT, when ATH is on the dawnside and MGD is at midnight. For the latitudinally separated stations (Figure 7e), the peak of occurrence rate is located around 20 UT when both stations are on the dawnside. This result suggests that Pc1 pulsations can propagate more easily to different stations in the nighttime because the plasma density in the *F* region of the ionosphere is lower at these times. In Figure 7c, the similarity of Pc1 pearl structures at the longitudinally separated stations shows that high-similarity events ($r > 0.7$) are concentrated between 6 and 15 UT when it is nighttime at both stations and, in particular, ATH is in the dawn sector and MGD in the midnight sector. However, in the case of latitudinally separated stations, as shown in Figure 7f, the similarity of Pc1 pearl structures is independent of UT.

Figure 8 shows the seasonal variations of the occurrence rate of Pc1 pulsations and the similarity of Pc1 pearl structures for the longitudinally and latitudinally separated stations. In both cases, we see that the highest occurrence rate of Pc1 pulsations at ATH, MGD, and MOS takes place near the equinoxes (peaks of occurrence in March and October), as shown in Figures 8a and 8b. The seasonal variations of Pc1 occurrence observed simultaneously at both stations are similar to those at each station. This result is consistent with those at high latitudes reported by *Fraser* [1968] and *Kuwashima et al.* [1981]. They reported that seasonal variations of Pc1 occurrence reach a maximum at equinoxes at high latitudes and in the winter at low latitudes due to ionospheric plasma density variations depending on the season, causing different attenuations of Pc1 waves during ionospheric duct propagation. As shown in Figures 8c and 8f, the similarity of Pc1 pearl structures in both cases is highly scattered and shows no seasonal dependence.

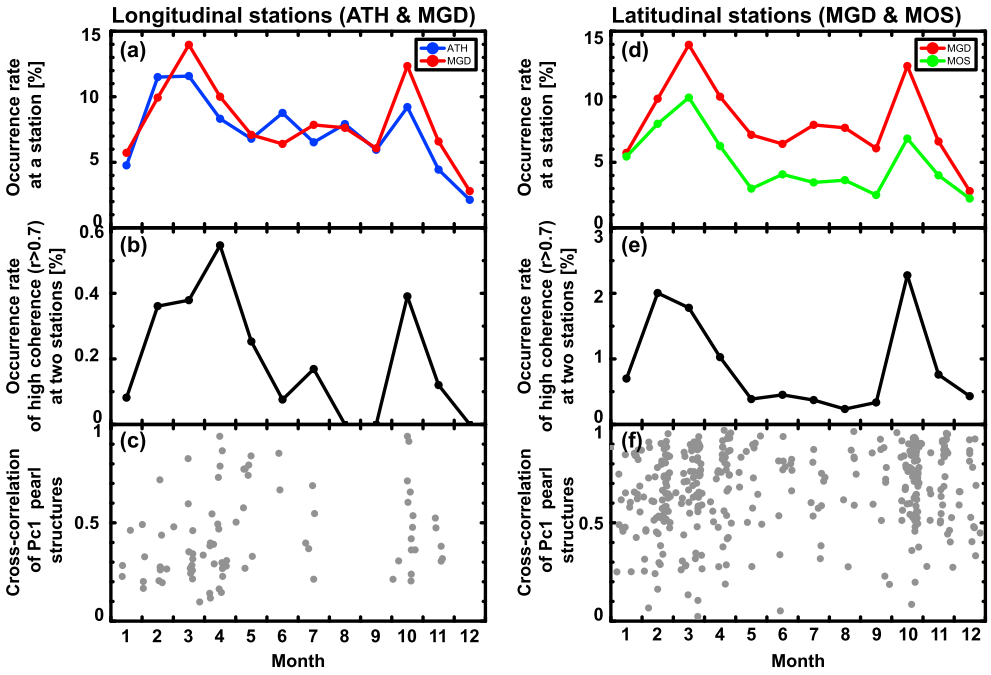

Figure 8. Seasonal variations of the Pc1 occurrence rate observed at each station, at the two stations, and the cross-correlation coefficient of Pc1 pearl structures for (a)–(c) longitudinally (ATH and MGD) and (d)–(f) latitudinally (MGD and MOS) separated stations, respectively.

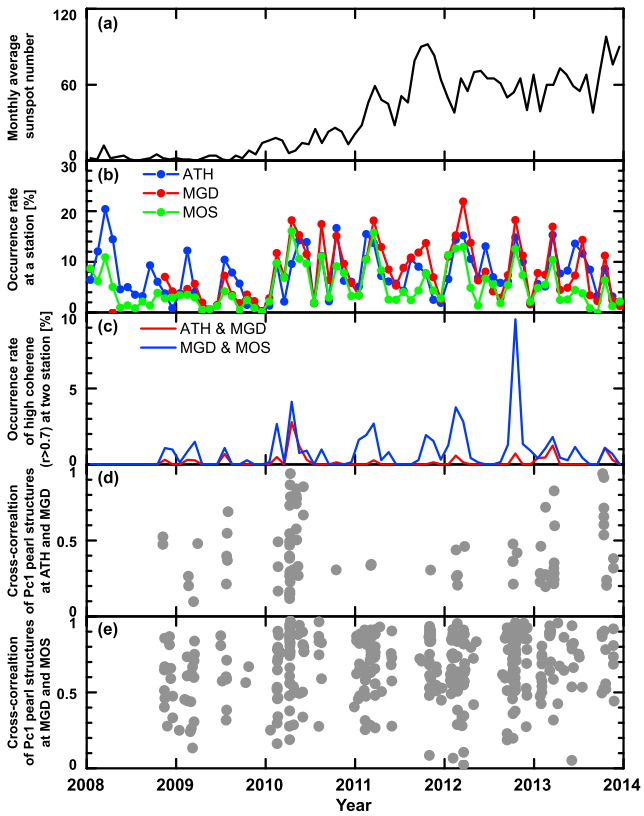

Figure 9. Annual variations of (a) monthly average sunspot number, the Pc1 occurrence rate observed (b) at ATH (blue line), MGD (red line) and MOS (green line), and (c) simultaneously at ATH and MGD (red line) and MGD and MOS (blue line), and cross-correlation coefficients of Pc1 pearl structures for (d) longitudinally separated (ATH and MGD) and (e) latitudinally separated (MGD and MOS) stations, from January 1, 2008, to December 31, 2013.

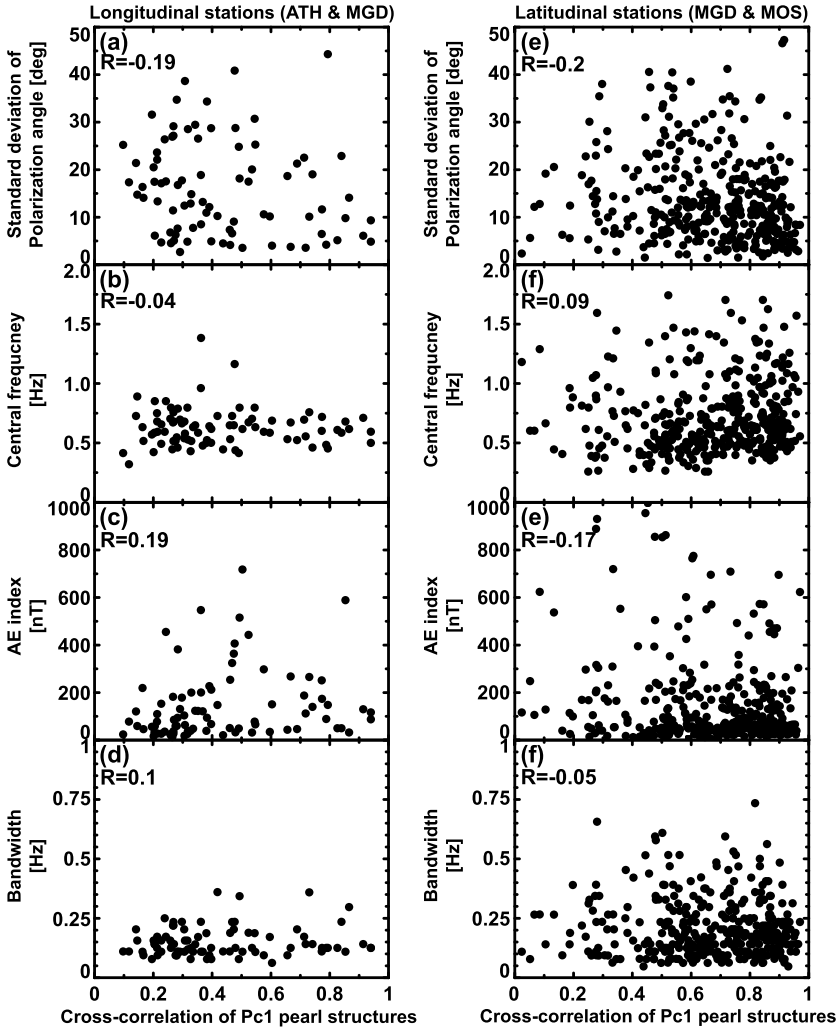

Figure 10. Dependence of the cross-correlation coefficient of Pc1 pearl structures on the standard deviation of Pc1 polarization angle, Pc1 central frequency, *AE* index, and Pc1 bandwidth, respectively, for (a)–(d) longitudinally (ATH and MGD) and (e)–(h) latitudinally (MGD and MOS) separated stations.

The annual variations of Pc1 occurrence and similarity of Pc1 pearl structures for the longitudinally and latitudinally separated stations are shown in Figure 9, together with monthly average sunspot number in Figure 9a. The sunspot numbers varied from minimum to maximum from 2008 to 2013. We observed fewer Pc1 events at these stations during the solar minimum than during the solar maximum, as shown in Figure 9b. The Pc1 occurrence at MGD (red line in Figure 9b) and MOS (green line in Figure 9b) seems to suddenly increase with increasing sunspot numbers until 2012 and then to decreases slightly in 2013. This result differs from those of previous studies [*Fraser-Smith*, 1970; *Kawamura et al.*, 1981; *Park et al.*, 2013], where it was reported that Pc1 occurrence has a negative correlation with sunspot number variations. As our ground observation covers only half of the solar cycle, we cannot investigate Pc1 activity over the variation of a full cycle; therefore, this subject will be investigated in future works. The annual variations of Pc1 occurrence at each station (Figure 9b) and longitudinally and latitudinally separated stations (Figure 9c) show clear seasonal variations. The similarity of Pc1 pearl structures in both pairs (Figures 9d and 9e) seems to be independent of year and sunspot variation.

3.3. Dependence of the Similarity of Pc1 Pearl Structures on Geomagnetic Conditions and Wave Properties

The relationships between the similarity of Pc1 pearl structures in the ionosphere and geomagnetic conditions and other wave properties are shown in Figure 10. Figures 10a–10d show the results for the longitudinally separated stations, and Figures 10e–10f show the results for the latitudinally separated stations. We calculated correlation coefficients *R* for these plots as noted in the top left of each panel. We investigated dependence of

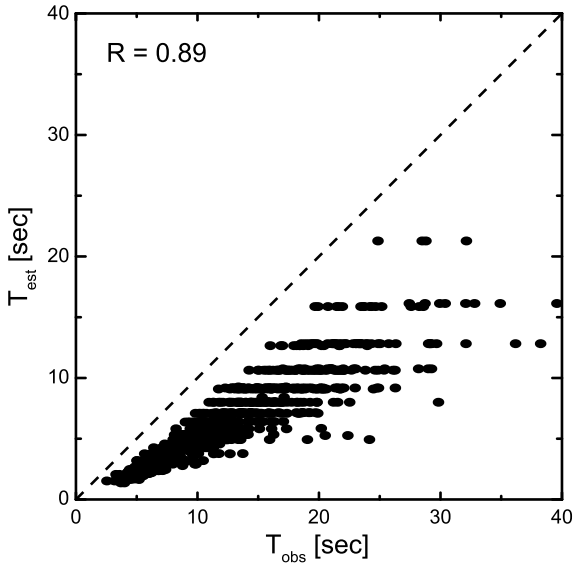

Figure 11. Scatterplot of observed repetition periods of Pc1 pearl structures versa the estimated beating periods at the three stations. The dashed line indicates the line of equality. *R* indicates the correlation coefficient between two values.

four parameters on the similarity of Pc1 pearl structures. The σ_θ represents the ionospheric source distribution, as shown in Figures 2c and 2d. The central frequency and bandwidth of Pc1 pulsations represent latitudes of the ionospheric source. If Pc1 waves are generated at the equatorial region of the magnetosphere and propagate along the magnetic field lines, their frequencies depend on the magnetic field intensity at the equatorial region. We consider that higher (lower) frequencies of Pc1 pulsations are related to the magnetic field at lower (higher) latitudes. The average *AE* index represents the total current intensity in the auroral ionosphere and thus the level of disturbance of ionospheric conditions.

The σ_θ in both pairs (Figure 10a and 10e) tends to have weak negative correlation with the similarity of Pc1 pearl structures. However, the coefficients (−0.19 for the longitudinally (Figure 10a) and −0.2 for the latitudinally (Figure 10b) separated stations) are small. We also found no relationships ($R \sim 0$) between the similarity of Pc1 pearl structures and wave properties (i.e., central frequency in Figures 10b and 10f and bandwidth in Figures 10d and 10f). In Figures 10c and 10e, the average *AE* index and the similarity of Pc1 pearl structures show weak positive and negative correlations for the longitudinally and latitudinally separated stations, respectively.

3.4. Dependence of the Pc1 Pearl Periods on Pc1 Bandwidth

If the Pc1 pearl structure is caused by the beating of Pc1 waves with slightly different frequencies during their duct propagation in the ionosphere, the repetition period of the pearl structure should have a relation to the frequency difference, i.e., bandwidth of the Pc1 waves. Namely, we can estimate the possible repetition period $T_{est} = 1/f_{beating}$ of Pc1 pearl structures using the observed Pc1 bandwidth, as described by the simple beating equation ($f_{beating} = f_{upper} - f_{lower}$), where f_{upper} and f_{lower} are upper and lower frequencies of the observed Pc1 band. We chose f_{upper} and f_{lower} using the boundary of the Pc1 band that satisfies our event selection criteria, which are Pc1 power higher than 10^{-7} nT^2/Hz and high coherence ($C > 0.7$) of Pc1 waveforms between the two stations (as shown in Figure 4). Figure 11 shows the relationship between observed and estimated repetition periods of Pc1 pearl structures at the three stations. We used all of the 84 and 370 Pc1 pearl structure events observed at three stations. We define the observed repetition periods of Pc1 pearl structures by calculating the time intervals between amplitude peaks of the pearl structures, as shown in the example in Figures 5a and 5b, and calculated the average repetition period T_{obs} for each event by averaging all the repetition periods during the ± 2 min intervals of the event.

In Figure 11, we found that averaged repetition periods of Pc1 pearl structures have a clear positive correlation ($R = 0.89$) with the estimated values. We also note that they are scattered always below the estimated repetition period from the Pc1 bandwidth. Since we took the frequencies of the upper and lower boundary of the Pc1 bandwidth to estimate T_{est}, we expect the actual beating period T_{obs} should be always larger than

the dashed line in Figure 11. Thus, the two facts that there is a clear positive correlation between T_{obs} and T_{est} and that the T_{obs} is always larger than T_{est}, strongly support the idea that the beating of Pc1 waves in their bandwidth creates the Pc1 pearl structures.

4. Discussion

In this study, we investigated the statistical characteristics of Pc1 pearl structures in the ionosphere using multipoint ground stations, with the aim of understanding possible mechanisms for the generation of Pc1 pearl structures in the ionosphere.

We found that more than half of Pc1 events observed at the longitudinally and latitudinally separated stations have low similarity ($r < 0.7$) for Pc1 pearl structures in Figure 6. If Pc1 pearl structures are mainly generated in the ionosphere, they should show different pearl structures at different stations, even though they came from a same source region. On the other hand, if Pc1 pearl structures are caused by magnetospheric effects, they should have a similar shape at different stations. Thus, the low similarity of Pc1 pearl structures at different stations suggests that ionospheric effects are the dominant generation mechanism for Pc1 pearl structures in the ionosphere. In addition, the positive correlation between the observed and estimated Pc1 repetition period in Figure 11 supports the idea that the beating of different frequency waves in the ionospheric duct creates the Pc1 pearl structures.

When Pc1 pulsations propagate a longer distance through the ionospheric duct, they would be more attenuated. Thus, stations located farther from the source region would observe weaker Pc1 pulsations. In that sense, we may not be able to exclude the possibility that local background noise becomes dominant for these waves, causing the low-similarity r of Pc1 pearl structures. In this study, however, we selected Pc1 events with wave power higher than 10^{-7} nT^2/Hz, which is the threshold for which the observed pearl structures can be clearly distinguished from background noise. To identify whether the influence of background noise contributes to the low similarity of Pc1 pearl structures at different stations, we investigated the dependence of the similarity r of Pc1 pearl structures on Pc1 power at each station in both pairs. The correlation coefficients between the pearl similarity and Pc1 wave power are 0.47 at ATH and 0.08 at MGD at the longitudinally separated stations and 0.14 at MGD and 0.15 at MOS at the latitudinally separated stations. These results indicate that the similarity r of Pc1 pearl structures has a weak positive correlation with Pc1 wave power at only ATH for the longitudinally separated stations. We conclude that background noise does not much affect on the similarity r of Pc1 pearl structures.

We investigated the temporal variations of the similarity of Pc1 pearl structures (Figures 7–9). For UT variation in Figure 7, high-similarity events at the longitudinally separated stations are detected only when both stations are located in the night sector. This result suggests that Pc1 pearl structures caused by magnetospheric effects are frequently observed in the nighttime of the magnetosphere. If this is the case, then latitudinally separated stations should also observe high-similarity events of Pc1 pearl structures in the nighttime. However, for the latitudinally separated stations, the similarity of Pc1 pearl structures is highly scattered at all UT. We also could not find any seasonal and annual variations in the similarity of Pc1 pearl structures as shown in Figures 8 and 9. The formation of Pc1 pearl structures seems to be independent of ionospheric conditions.

We note that the similarity of Pc1 pearl structures has a weak negative correlation with the standard deviation of the polarization angle in both cases. Although it is small, this negative correlation supports the idea that Pc1 waves coming from a spatially distributed source can generate different Pc1 pearl structures at different observation points by beating processes in the ionosphere. *Nomura et al.* [2011] suggested that Pc1 polarization angle has dependence on frequency. *Sakaguchi et al.* [2008] reported that the isolated proton auroral spots, indicators of Pc1 ionospheric sources, were intermittently distributed over a 4 h magnetic local time period in the premidnight sector equatorward of the substorm auroral activity at auroral latitudes. *Jun et al.* [2014] noted that Pc1 pulsations having a polarization angle dependence on Pc1 frequency have differently shaped Pc1 pearl structures at different stations.These observations indicate that if Pc1 pulsations come from distributed ionospheric source regions, they could have different Pc1 pearl structures at different observation points due to different propagation time delays from the source regions to the ground stations.

Although the negative correlation between σ_θ and the pearl similarity r support the idea that Pc1 waves coming from a spatially distributed source cause beating and thus Pc1 pearl structure, the absolute value of the correlation is small (~0.2). This may be because of the effect of relative location of the ground station to the

ionospheric source region. If the ionospheric source region is too close to the stations, the polarization angle θ shows complex patterns, as a mixture of direct incident Alfvén waves and ducting compressional waves. Thus, near the ionospheric source region, the minor (not major) axis of polarization angle can point to the source region [*Fujita and Tamao*, 1988; *Nomura et al.*, 2012]. This effect would contribute to reduce the correlation between σ_θ and the similarity r.

In our study, other parameters (i.e., central frequency, bandwidth, and *AE* index) did not have any correlation with the similarity of Pc1 pearl structures. We supposed that lower frequency Pc1 pulsations may have longer propagation time than that of higher frequency because they come from higher latitudes, resulting that lower frequency waves may be more attenuated during the ionospheric duct propagation. Thus, if the central frequency has a positive correlation with the Pc1 pearl similarity, Pc1 pearl similarity may be related to the attenuation effect. Our result shows, however, that Pc1 pearl similarity has no clear correlation with the central frequency and bandwidth. For the *AE* dependence in Figures 10c and 10e, if attenuation effect is controlled by the ionospheric condition represented by *AE* index, the similarity of Pc1 pearl structures should have a negative correlation with *AE* index. Our result shows, however, that there is no clear relationship between Pc1 pearl generation and *AE* index.

5. Conclusion

We investigated the statistical characteristics of Pc1 pearl structures observed by induction magnetometers at three ground stations (ATH, MGD, and MOS), located at midlatitude to low latitude, from 2008 to 2013. We selected 84 Pc1 events observed simultaneously at longitudinally separated stations and 370 events at latitudinally separated stations. The results of this study can be summarized as follows:

1. The cross-correlation coefficients $r(\Delta t)$ for pearl structure similarities have a peak of occurrence at ~0.2 for the longitudinally separated stations (ATH and MGD) and at ~0.8 for the latitudinally separated stations (MGD and MOS). More than half of the events in both pairs (69 events at the longitudinally separated stations and 178 at the latitudinally separated stations) have a similarity of pearl structures less than 0.7, suggesting that ionospheric effects could be the dominant generation mechanism for Pc1 pearl structures in the ionosphere.
2. High-similarity Pc1 pearl structures ($r > 0.7$) at the longitudinally separated stations are concentrated from 6 to 15 UT when it is nighttime at both stations. We could not find any seasonal or annual dependence in the similarity of Pc1 pearl structures.
3. Pc1 occurrences at all stations have a peak in the daytime during equinox periods. However, Pc1 pulsations observed simultaneously at two stations in both pairs are frequently detected in the dawn sector, indicating that the dawn sector and equinox period provide favorable conditions for propagation of Pc1 pulsations through the ionospheric duct.
4. The similarity of Pc1 pearl structures tends to have weak negative correlation with the standard deviation of the polarization angle ($R \sim 0.2$) in both cases (longitudinally and latitudinally separated stations). However, we found that the similarity of Pc1 pearl structures is less correlated (or has less correlation) with central frequency and bandwidth at longitudinally and latitudinally separated stations. If we take into account the *AE* index, in both cases, the correlation coefficient between *AE* and Pc1 similarity has the same absolute value but is positive for the longitudinal case and negative for latitudinally separated stations. Thus, we could not find any relationship between the similarity of Pc1 pearl structures and other parameters (central frequency, bandwidth, and *AE* index).
5. There is a clear positive correlation between the observed Pc1 repetition periods with the periods estimated from the Pc1 bandwidth by considering the beating. The observed repetition period is always larger than the estimated period.

From these results, we conclude that ionospheric effects, particularly the beating of different frequency waves, could be the dominant mechanism for Pc1 pearl structures in the ionosphere. We also suggest that the different shapes of Pc1 pearl structures at different points could be mainly by the beating in the ionosphere with a spatially extended ionospheric source during ionospheric duct propagation. High-similarity events of Pc1 pearl structures are also observed at both longitudinally and latitudinally separated stations. Thus, we should also consider that magnetospheric processes, such as EMIC waves modulated by long period ULF waves, could have a contribution in the generation of Pc1 pearl structures. To understand and quantify the

contributions to the creation of Pc1 pearl structures in the ionosphere and in the magnetosphere, we would like to investigate the statistical propagation characteristics of Pc1 pearl structures using conjugate ground-satellite observations in future studies.

Acknowledgments

We thank M. Sera and Y. Ikegami at the Moshiri observatory of the Institute for Space-Earth Environmental Research, Nagoya University, and the staff of the Institute of Cosmophysical Research and Radiowave Propagation (IKIR) and of the Center for Science, Athabasca University. We also thank Y. Katoh, H. Hamaguchi, and Y. Yamamoto of ISEE for their help and support in the operation of the induction magnetometers. The induction magnetometer data are available at the magnetometer data website from the Institute for ISEE accessible at http://stdb2.stelab.nagoya-u.ac.jp/magne/index.html. The monthly average sunspot numbers were sourced from the OMNI database. The OMNI data were obtained from the SPDF/Goddard Space Flight Center interface at http://omniweb.gsfc.nasa.gov/. The *AE* indices were provided by the WDC-C2 for geomagnetism at Kyoto University at http://wdc.kugi.kyoto-u.ac.jp/. This work was supported by KAKENHI grants (16403007, 18403011, 19403010, 25247080, 20244080, 15H05815, and 16H06286), the Special Funds for Education and Research (Energy Transport Processes in Geospace), and the IUGONET Project from MEXT, Japan, as well as the Leadership Development Program for Space Exploration and Research from Nagoya University for Leading Graduate Schools.

References

Althouse, E. L., and J. R. Davis (1978), Five-station observations of Pc 1 micropulsation propagation, *J. Geophys. Res.*, *83*, 132–144.

Altman, C., and E. Fijalkow (1980), The horizontal propagation of Pc1 pulsations in the ionosphere, *Planet. Space Sci.*, *28*, 61–68.

Anderson, B., R. Denton, G. Ho, D. Hamilton, S. Fuselier, and R. Strangeway (1996), Observational test of local proton cyclotron instability in the Earth's magnetosphere, *J. Geophys. Res.*, *101*, 21,527–21,543.

Campbell, W. H. (1967), Low attenuation of hydromagnetic waves in the ionosphere and implied characteristics in the magnetosphere for Pc 1 events, *J. Geophys. Res.*, *72*, 3429–3445.

Erlandson, R., L. Zanetti, T. Potemra, L. Block, and G. Holmgren (1990), Viking magnetic and electric field observations of Pc 1 waves at high latitudes, *J. Geophys. Res.*, *95*, 5941–5955.

Fowler, R., B. Kotick, and R. Elliott (1967), Polarization analysis of natural and artificially induced geomagnetic micropulsations, *J. Geophys. Res.*, *72*, 2871–2883.

Fraser, B. (1968), Temporal variations in Pc1 geomagnetic micropulsations, *Planet. Space Sci.*, *16*, 111–124.

Fraser, B. (1975a), Ionospheric duct propagation and Pc 1 pulsation sources, *J. Geophys. Res.*, *80*, 2790–2796.

Fraser, B. (1975b), Polarization of Pc 1 pulsations at high and middle latitudes, *J. Geophys. Res.*, *80*, 2797–2807.

Fraser-Smith, A. (1970), Some statistics on Pc 1 geomagnetic micropulsation occurrence at middle latitudes: Inverse relation with sunspot cycle and semi-annual period, *J. Geophys. Res.*, *75*, 4735–4745.

Fujita, S. (1987), Duct propagation of a short-period hydromagnetic wave based on the international reference ionosphere model, *Planet. Space Sci.*, *35*, 91–103.

Fujita, S. (1988), Duct propagation of hydromagnetic waves in the upper ionosphere: 2. Dispersion characteristics and loss mechanism, *J. Geophys. Res.*, *93*, 14,674–14,682.

Fujita, S., and T. Tamao (1988), Duct propagation of hydromagnetic waves in the upper ionosphere, 1. Electromagnetic field disturbances in high latitudes associated with localized incidence of a shear Alfvén wave, *J. Geophys. Res.*, *93*, 14,665–14,673.

Fukunishi, H., T. Toya, K. Koike, M. Kuwashima, and M. Kawamura (1981), Classification of hydromagnetic emissions based on frequency-time spectra, *J. Geophys. Res.*, *86*, 9029–9039.

Greifinger, C., and P. S. Greifinger (1968), Theory of hydromagnetic propagation in the ionospheric waveguide, *J. Geophys. Res.*, *73*, 7473–7490.

Guglielmi, A., F. Feygin, K. Mursula, J. Kangas, T. Pikkarainen, and A. Kalisher (1996), Fluctuations of the repetition period of Pc1 pearl pulsations, *Geophys. Res. Lett.*, *23*, 1041–1044.

Hino, M. (1977), *Spectral Analysis*, Asakura, Tokyo.

Horne, R. B., and R. M. Thorne (1993), On the preferred source location for the convective amplification of ion cyclotron waves, *J. Geophys. Res.*, *98*, 9233–9247.

Hu, Y., and R. Denton (2009), Two-dimensional hybrid code simulation of electromagnetic ion cyclotron waves in a dipole magnetic field, *J. Geophys. Res.*, *114*, A12217, doi:10.1029/2009JA014570.

Jacobs, J., and T. Watanabe (1964), Micropulsation whistlers, *J. Atmos. Terr. Phys.*, *26*, 825–826.

Jun, C.-W., K. Shiokawa, M. Connors, I. Schofield, I. Poddelsky, and B. Shevtsov (2014), Study of Pc1 pearl structures observed at multi-point ground stations in Russia, Japan, and Canada, *Earth Planet. Space*, *66*, 1–14.

Kawamura, M., M. Kuwashima, and T. Toya (1981), Comparative study of magnetic Pc1 pulsations between low latitudes and high latitudes: Source region and propagation mechanism of the waves deduced from the characteristics of the pulsations at middle and low latitudes, in *The Third Symposium on Coordinated Observations of the Ionosphere and the Magnetosphere in the Polar Regions, Mem. of Natl. Inst. of Polar Res. Spec. Issue*, vol. 18, edited by T. Nagata, pp. 83–100, Natl. Inst. of Polar Res., Tokyo.

Kim, H., M. Lessard, M. Engebretson, and H. Lühr (2010), Ducting characteristics of Pc 1 waves at high latitudes on the ground and in space, *J. Geophys. Res.*, *115*, A09310, doi:10.1029/2010JA015323.

Kim, H., M. Lessard, M. Engebretson, and M. Young (2011), Statistical study of Pc1-2 wave propagation characteristics in the high-latitude ionospheric waveguide, *J. Geophys. Res.*, *116*, A07227, doi:10.1029/2010JA016355.

Kuwashima, M., T. Toya, M. Kawamura, T. Hirasawa, H. Fukunishi, and M. Ayukawa (1981), Comparative study of magnetic Pc1 pulsations between low latitudes and high latitudes: Statistical study, in *The Third Symposium on Coordinated Observations of the Ionosphere and the Magnetosphere in the Polar Regions, Mem. of Natl. Inst. of Polar Res. Spec. Issue*, vol. 18, edited by T. Nagata, pp. 101–117, Natl. Inst. of Polar Res., Tokyo.

Lysak, R. (2004), Magnetosphere-ionosphere coupling by Alfvén waves at midlatitudes, *J. Geophys. Res.*, *109*, A07201, doi:10.1029/2004JA010454.

Manchester, R. (1966), Propagation of Pc 1 micropulsations from high to low latitudes, *J. Geophys. Res.*, *71*, 3749–3754.

Manchester, R. (1970), Propagation of hydromagnetic emissions in the ionospheric duct, *Planet. Space Sci.*, *18*, 299–307.

Mursula, K. (2007), Satellite observations of Pc 1 pearl waves: The changing paradigm, *J. Atmos, Sol. Terr. Phys.*, *69*(14), 1623–1634.

Mursula, K., R. Rasinkangas, T. Bösinger, R. Erlandson, and P.-A. Lindqvist (1997), Nonbouncing Pc 1 wave bursts, *J. Geophys. Res.*, *102*, 17,611–17,624.

Mursula, K., J. Kangas, R. Kerttula, T. Pikkarainen, A. Guglielmi, O. Pokhotelov, and A. Potapov (1999), New constraints on theories of Pc1 pearl formation, *J. Geophys. Res.*, *104*, 12,399–12,406.

Mursula, K., T. Bräysy, K. Niskala, and C. Russell (2001), Pc1 pearls revisited: Structured electromagnetic ion cyclotron waves on Polar satellite and on ground, *J. Geophys. Res.*, *106*, 29,543–29,553.

Nakamura, S., Y. Omura, S. Machida, M. Shoji, M. Nosé, and V. Angelopoulos (2014), Electromagnetic ion cyclotron rising tone emissions observed by THEMIS probes outside the plasmapause, *J. Geophys. Res. Space Physics*, *119*, 1874–1886, doi:10.1002/2013JA019146.

Nomura, R., K. Shiokawa, V. Pilipenko, and B. Shevtsov (2011), Frequency-dependent polarization characteristics of Pc1 geomagnetic pulsations observed by multipoint ground stations at low latitudes, *J. Geophys. Res.*, *116*, A01204, doi:10.1029/2010JA015684.

Nomura, R., K. Shiokawa, K. Sakaguchi, Y. Otsuka, and M. Connors (2012), Polarization of Pc1/EMIC waves and related proton auroras observed at subauroral latitudes, *J. Geophys. Res.*, *117*, A02318, doi:10.1029/2011JA017241.

Omura, Y., J. Pickett, B. Grison, O. Santolik, I. Dandouras, M. Engebretson, P. M. Décréau, and A. Masson (2010), Theory and observation of electromagnetic ion cyclotron triggered emissions in the magnetosphere, *J. Geophys. Res.*, *115*, A07234, doi:10.1029/2010JA015300.

Park, J., H. Lühr, and J. Rauberg (2013), Global characteristics of Pc1 magnetic pulsations during solar cycle 23 deduced from CHAMP data, *Ann. Geophys.*, *31*, 1507–1520.

Paulson, K., C. Smith, M. Lessard, M. Engebretson, R. Torbert, and C. Kletzing (2014), In situ observations of Pc1 pearl pulsations by the Van Allen Probes, *Geophys. Res. Lett.*, *41*, 1823–1829, doi:10.1002/2013GL059187.

Perraut, S. (1982), Wave-particle interactions in the ULF range: GEOS-1 and -2 results, *Planet. Space Sci.*, *30*, 1219–1227.

Pope, J. H. (1964), An explanation for the apparent polarization of some geomagnetic micropulsations (pearls), *J. Geophys. Res. Space Physics*, *69*, 399–405.

Rasinkangas, R., and K. Mursula (1998), Modulation of magnetospheric EMIC waves by Pc 3 pulsations of upstream origin, *Geophys. Res. Lett.*, *25*, 869–872.

Sakaguchi, K., K. Shiokawa, Y. Miyoshi, Y. Otsuka, T. Ogawa, K. Asamura, and M. Connors (2008), Simultaneous appearance of isolated auroral arcs and Pc 1 geomagnetic pulsations at subauroral latitudes, *J. Geophys. Res.*, *113*, A05201, doi:10.1029/2007JA012888.

Shiokawa, K., et al. (2010), The STEL induction magnetometer network for observation of high-frequency geomagnetic pulsations, *Earth Planets Space*, *62*, 517–524.

Shoji, M., and Y. Omura (2013), Triggering process of electromagnetic ion cyclotron rising tone emissions in the inner magnetosphere, *J. Geophys. Res. Space Physics*, *118*, 5553–5561, doi:10.1002/jgra.50523.

Tepley, L., and R. Landshoff (1966), Waveguide theory for ionospheric propagation of hydromagnetic emissions, *J. Geophys. Res.*, *71*, 1499–1504.

Troitskaya, V., and A. Gul'Elmi (1967), Geomagnetic micropulsations and diagnostics of the magnetosphere, *Space Sci. Rev.*, *7*, 689–768.

Usanova, M., I. Mann, I. Rae, Z. Kale, V. Angelopoulos, J. Bonnell, K.-H. Glassmeier, H. Auster, and H. Singer (2008), Multipoint observations of magnetospheric compression-related EMIC Pc1 waves by THEMIS and CARISMA, *Geophys. Res. Lett.*, *35*, L17S25, doi:10.1029/2008GL034458.

Waters, C., R. Lysak, and M. Sciffer (2013), On the coupling of fast and shear Alfvén wave modes by the ionospheric hall conductance, *Earth Planets Space*, *65*, 385–396.